Computers and Concrete, Vol. 2, No. 3 (2005) 177-188
DOI: http://dx.doi.org/10.12989/cac.2005.2.3.177

Inelastic analysis of concrete beams strengthened with various fiber reinforced polymer (FRP) systems

M. J. Terro†

Civil Engineering Department, Kuwait University, Kuwait

M. M. El-Hawary‡

Kuwait Institute for Scientific Research, Kuwait

S. A. Hamoush‡†

Architectural Engineering, Department, A & T State University, Greensboro, NC, USA

(Received October 27, 2004, Accepted May 2, 2005)

Abstract. This paper presents a numerical model developed to evaluate the load-deflection and moment-curvature relationship for concrete beams strengthened externally with four different Fiber Reinforced Polymer (FRP) composite systems. The developed model considers the inelastic behavior of concrete section subjected to a combined axial force and bending moment. The model accounts for tensile strength of concrete as defined by the modulus of rupture of concrete. Based on the adopted material constitutive relations, the model evaluates the sectional curvature as a function of the applied axial load and bending moment. Deflections along the beam are evaluated using a finite difference technique taking into account support conditions. The developed numerical technique has been tested on a cantilever beam with a transverse load applied at its end. A study of the behavior of the beam with tension reinforcement compared to that with FRP areas giving an equivalent ultimate moment has been carried out. Moreover, cracking of the section in the tensile region at ultimate load has also been considered. The results indicated that beams reinforced with FRP systems possess more ductility than those reinforced with steel. This ductility, however, can be tuned by increasing the area of FRP or by combining different FRP layers.

Keywords: reinforced concrete; fiber reinforcement; flexure; finite difference; nonlinear behavior.

1. Introduction

During recent years, interest in the nonlinear analysis of concrete members has increased steadily because of the need for better understanding of their actual behavior leading to a better implementation at optimum capacity. Exact analytical solutions to the materially nonlinear behavior of concrete do not exist. Such closed-form solutions based on elastic-perfectly plastic assumptions were introduced for special problems only. Therefore, numerical solutions tools are

† Associate Professor
‡ Research Scientist, mhawary@safat.kisr.edu.kw
‡† Assistant Professor

usually sought to provide an actual analysis in the nonlinear range. The most popular solutions are the finite element (FEM), the equivalent system, the secant stiffness, and the cell discretization methods.

The first application of the FEM to RC structures dates back to the late 1960s. Since then, rapid and great advances have been recorded, as can be seen in several comprehensive articles in the literature. Reinforced concrete exhibits a very complex behavior near ultimate loads. The complexity of this behavior can be observed in the nonlinear multi-axial stress-strain response, tensile cracking, compressive crushing, material failures, and strain softening. Furthermore, the composite nature of the material introduces additional difficulties in modeling the interactions between reinforcement and concrete. Each aspect of the material behavior requires special and extensive attention. Several alternative approaches and constitutive relations have been suggested (Rasheed and Dinno 1994, Ngo and Scordelis 1994), but no general universal agreement has been reached. An incremental-iterative analysis algorithm using the secant stiffness approach was developed by Rashid and Dinno (1994). They succeeded in a direct prediction of the nonlinear behavior of RC rectangular sections coupled with relevant flexural and axial rigidities. Although this model takes into account the axial loads, it failed to provide inelastic deflection along the member.

Vecchio (1989) modified existing linear finite element routines to enable a nonlinear analysis. This procedure was based on an iterative, secant stiffness formulation and employed constitutive relations for concrete and reinforcement based on the modified compression field theory.

Pagnoni and Slater (1992) developed a constitutive relation for reinforced concrete by combining the bounding surface model with numerical procedures for the modeling of crack propagation. Tension stiffening and steel reinforcement interaction effects were modeled by a constitutive bounding surface model.

Although many of these researchers have used the finite element technique for the nonlinear analysis of RC, there is a number of factors that prevented a wider acceptability of this method. The first important consideration is that the constitutive properties of concrete have not been identified completely. There are still no general accepted material laws available to model actual concrete behavior. Non-linear finite element analysis of concrete structures can be very costly since it requires considerable structural and numerical experience.

Other researchers have used different approaches for the nonlinear analysis of concrete like the one by Fertis, who proposed the equivalent systems method (Fertis and Zobel 1958, 1961). This method was used to analyze non-prismatic elastic sections. In this method, stress and deflection characteristics of members are determined by replacing the original member of variable stiffness with one of uniform stiffness, whose elastic line is identical to the original variable stiffness member. The method was further improved to include the non-elastic behavior of material (Fertis and Keene 1990, Fertis and Tanej 1991). This method, however, is not suitable for analyzing sections subjected to combined axial and transverse loads.

Auciello and Ercolano (1992) have proposed the cell discretization technique to analyze large deflections of beams characterized by a cubic constitutive equation. The solution was obtained by means of an energy process using cell discretization. The system of nonlinear equations was solved with a suitable combination of the Newton and Gauss-Seidel methods.

Hamoush and Terro (1993) developed an exact solution model for sections subjected to combined axial force and bending moment. The load-strain relation was developed for six different modes of strain: pure elastic, pure plastic and elastic-plastic in compression and tension. A Newton-Raphson

concept was used in the iteration technique for determining the strain values ε_1 at the top and ε_2 at the bottom surfaces of section. However, that model was proposed for steel members only.

The performance of reinforced concrete members under load depends, to a great extent, on the stress-strain relationship of concrete and steel and on the type of stress applied.

The constitutive modeling of concrete has received a worldwide research attention in the literature. Many researchers have proposed empirical functions for the stress-strain relation of concrete in compression (Wang, *et al*. 1978, Ahmad and Shah 1979). The work presented by Desayi and Krishan (1964) and modified by Tsai (1987) has formed the basis of the constitutive modeling employed in this paper.

The use of Fiber Reinforced Polymers FRP in reinforced concrete structures is gaining a worldwide acceptance due to their numerous advantages. FRP are easy to handle, light weight, posses high tensile strength and excellent resistance to fatigue, chemicals and corrosion.

The research work on FRP laminates includes that on ductility of strengthened beams (El-Hawary, *et al*. 2003, Bencardino, *et al*. 2002, Duthinh and Starnes 2004); importance of adequate anchorage system (Spadea 2000); effect of CFRP on concrete confinement (Swamy and Mukhopadhyaya 1999); effect of FRP configuration on behavior (Brena and Macri 2004) and modeling of FRP confined concrete (Javier Malvar, *et al*. 2004, Fujikake, *et al*. 2004). ACI 440 report (1996) contains also some details regarding the use of FRP in concrete structures.

FRP may also be used as strands for internal reinforcement replacing steel bars in reinforced concrete structures (Hamid, *et al*. 1995).

The nonlinear behavior of concrete in compression and tension are both considered in the work presented in this paper. The load-deflection and moment-curvature behavior of a typical cantilever with a point transverse load at its end is analyzed. A comparison between the behavior of the beam with tensile steel reinforcement and that with Fiber Reinforced Polymer (FRP) is presented. Four different types of FRP systems are employed in this analysis: Nonlinear and linear systems incorporating glass fibers and nonlinear and linear systems incorporating carbon fibers. The authors are also in the process of introducing additional FRP types for the replacement of tension steel in the repair of RC structures. The areas of FRP used in the analysis were calculated such that their ultimate moment is equivalent to that of a beam with steel tension reinforcement only. Since the behavior of concrete in tension is also included, patterns of cracking giving zero tension in concrete were also taken into account in the numerical method. A simplified finite difference technique is employed to determine the load-deflection characteristics along the beam, taking into account its support conditions. The computer code for the model has been developed using MATLAB (2002).

The constitutive relations adopted for concrete and reinforcing steel in addition to those of the employed FRP systems are presented in this work. Different values of the point transverse load are studied up to the failure value giving an ultimate moment at the support. Cracking patterns are considered at the failure load only. The results indicated that beams reinforced with FRP systems possess more ductility than those reinforced with steel. This is expected since the moduli of elasticity of all four types of FRP are much lower than that of reinforcing steel. Should a lower ductility be required, an optimum value of FRP area for one or combination of FRP layers could be employed.

2. Constitutive stress-strain relations

2.1. Concrete

Although tensile stresses in concrete are very small, they can be relatively significant at low values of loading. This is why the proposed model adopted in compression the relations developed by Desayi and Krishan (1964) and modified by Tsai (1987), and extended it to tension. This constitutive relation is presented in the equation below and illustrated in Fig. 1:

$$f_c = 2f''_c \frac{(\varepsilon_c / \varepsilon_0)}{1 + (\varepsilon_c / \varepsilon_0)^2} \tag{1}$$

Where; $\varepsilon_0 = 1.71 \frac{f'_c}{E_c}$ and $f''_c = 0.9f'_c$

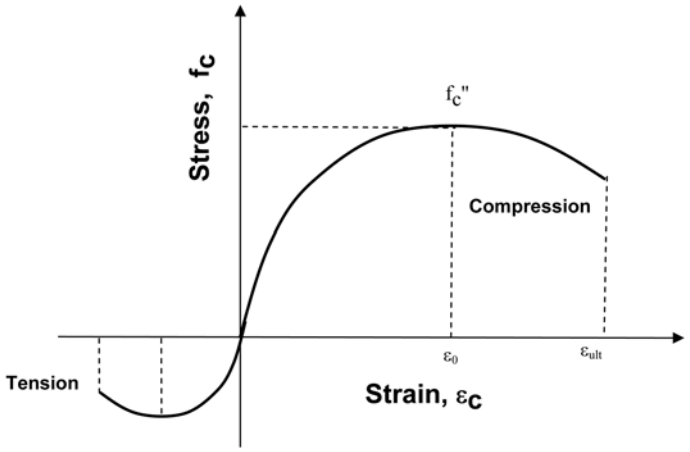

Fig. 1 Proposed stress-strain in compression and tension relation for concrete

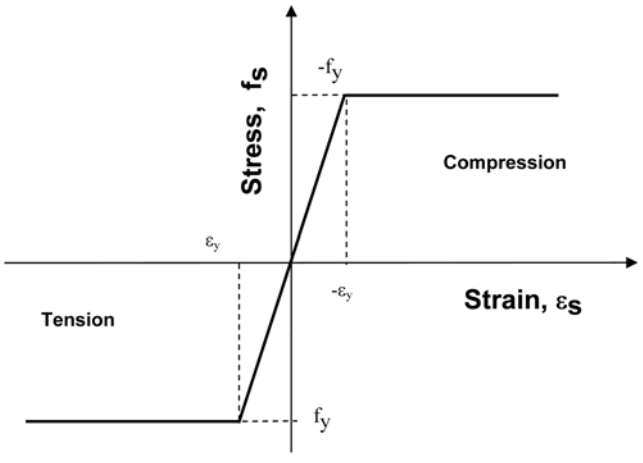

Fig. 2 Proposed stress-strain in compression and tension relation for reinforcing steel

2.2. Reinforcing steel

A bilinear relation, elastic-perfectly plastic, for steel is considered in compression and tension. This relation is given in the equation below and illustrated in Fig. 2:

$$\sigma = E \times \varepsilon \qquad \text{for } E = 200 \text{ GPa} \qquad (2)$$

2.3. FRP systems

The FRP systems utilized in this work is based on woven glass or carbon fabric composites made of vinylester matrices. Vinylester is generally preferred over epoxy for its better resistance to moisture, strong fiber-matrix interface bond, interface durability and its usually cheaper in cost. The fabrics were used both on 0 and 45 degrees orientation, where 0 degree means that the load direction is parallel to the weft or weaving direction. The materials were tested experimentally by Hamoush (2001). The 0 degrees materials demonstrated linear response, while the 45 degrees loading showed high nonlinearity. The Ramberg-Osgood equation was selected to represent the behavior of the fabrics as it covers both linear and nonlinear responses of materials.

The constitutive relations for the four different types of FRP employed in this work are given in Eqs. (3) through (6) below Hamoush (2001). They are also illustrated in Fig. 3:

Linear glass fiber

$$\sigma = E \times \varepsilon \qquad \text{for } \varepsilon \leq 1.25\% \text{ and } E = 27.6 \text{ GPa} \qquad (3)$$

Linear carbon fiber

$$\sigma = E \times \varepsilon \qquad \text{for } \varepsilon \leq 1.25\% \text{ and } E = 48.3 \text{ GPa} \qquad (4)$$

Non-linear glass fiber

$$\varepsilon = \frac{\sigma}{E} + \left(\frac{\sigma}{R}\right)^{n}$$

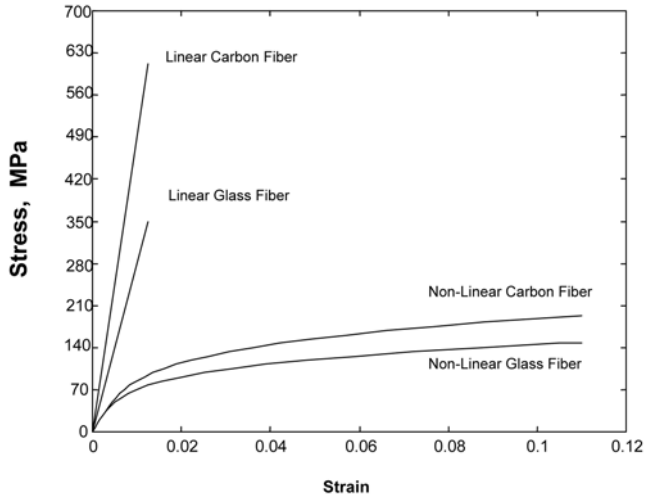

Fig. 3 Stress-strain relation for the four FRP systems in tension

for $\varepsilon \leq 11\%$ and $E = 11.7$ GPa; $R = 255.1$ GPa & $n = 4.2$ (5)

Non-linear carbon fiber

$$\varepsilon = \frac{\sigma}{E} + \left(\frac{\sigma}{R}\right)^{n}$$

for $\varepsilon \leq 11\%$ and $E = 11.7$ GPa; $R = 334.4$ GPa & $n = 4.2$ (6)

3. Finite difference approach

Deflections along the beam are calculated using the finite difference technique. In this finite difference solution, the member is divided into a number of equal elements. The elements are joined at their ends by nodes. A trial deflected shape is assumed to start the iterative method. The deflections are then calculated at the nodes using a Taylor approximation for beam-columns. The curvatures at nodes are calculated from internal equilibrium. The finite relationship between curvature and deflection is presented below. See reference (Desayi and Krishnan 1964)

$$\Delta_{i+1} = (l_{xx})\rho_i + 2\Delta_i - \Delta_{i-1} \tag{7}$$

where,

l_{xx} = length of each element or segment

Δ_i = displacement of loaded beam at node (i), measured from its initial position

ρ_i = curvature of section at node (i)

As can be seen from Eq. (7), a knowledge of two previous values of deflection is required to get that at node $i + 1$. If the beam is simply supported, a value is assumed at the middle of the beam-column, which would form node i. From symmetry, node $i - 1$ and node $i + 1$ would then have the same value. In which case, Eq. (7) would become as follows:

$$\Delta_{i+1} = ((l_{xx})\rho_i + 2\Delta_i) / 2 \tag{8}$$

Eq. (8), however, should only be used for the node next to the middle one. Knowing the assumed displacement at the middle and at the node next to it, the remaining deflection values should then be determined using Eq. (7) until the node at the simple support is reached. Since the deflection at the support should be equal to zero, the assumed value at the middle of the beam is then altered accordingly.

As for a cantilever beam-column case, the finite difference calculation is started at the fixed end. To satisfy a zero displacement and rotation at the fixed end, an imaginary node beyond the support with displacement $\Delta_{i-1} = \Delta_{i+1}$ is assumed. Since the displacement at the fixed end Δ_i is also equal to zero, Eq. (7) is written for the next node only as follows:

$$\Delta_{i+1} = (l_{xx})\rho_i / 2 \tag{9}$$

The deflection at the rest of the nodes are then calculated using Eq. (7). No iteration is required for the cantilever case.

4. Numerical algorithm

The computer code has been written using MATLAB (2002). This well-established and robust numerical tool will allow the authors to develop the presented methods further. The following steps has been followed throughout the analysis:

Step1 The beam-column is subdivided into n elements joined at their ends by n+1 nodes.

Step2 Starting at the fixed end, the moment and axial force are calculated at the section of each node.

Step3 With the strain at the compression side of the section fixed, the strain at the tension face is varied until equilibrium is reached between applied and calculated axial forces. Cracking patterns can be imposed by the user at desired nodes at the start of the analysis. If a crack is imposed at a section, the tension force in concrete is set to zero.

Step4 The strain at the compression face is, then, varied until the difference between applied and calculated moment changes sign and then iterated until it reaches acceptable user preset tolerances. It should be kept in mind that forces equilibrium in step 3 is performed and the strain at the tension face obtained whenever the strain at the compression face is varied.

Step 5 Having the strain values at both faces of the section at the node, the curvature is then obtained from the ratio of the difference between those two strain to the depth of the section.

Step 6 Next, Eq. (7) is employed to get the deflection at the next node. As mentioned above, the algorithm is first started by calculating the curvature at the fixed end to get the displacement at the next node using Eq. (9).

5. Numerical examples

The developed method has been tested for a simplified cantilever beam-column case where a hand verification of the results has been performed by the authors to check the accuracy of the results. The considered beam has a length of 3 m, and a 300×600 mm $\times$ mm concrete section with a compression steel of 2580 mm^2. A 76 mm concrete cover has been used for the compression and tension steel or FRP tension reinforcements. The concrete had a compressive strength of 27.58 MPa and the steel has a yield strength of 276 MPa. In the case of tensile steel reinforcement, a tensile steel area of 1290 mm^2 has been used, giving an ultimate moment of 264.45 kN.m.

To obtain the same ultimate moment value using FRP systems as a replacement for the tension reinforcing steel, the following areas of FRP were calculated:

Linear Glass Fiber = 1677.3 mm^2
Linear Carbon Fiber = 967.7 mm^2
Non-Linear Glass Fiber = 6276.8 mm^2
Non-Linear Carbon Fiber = 5025.3 mm^2

FRP fabrics were cut along the weft and on 45 degrees orientation to represent the linear and nonlinear cases, respectively. Although the nonlinear case does not provide optimum strengthening, the use of FRP at exactly 0° is not guaranteed in practice and hence the extreme, 45°, case has to be studied. The fabrics were fixed in place, using epoxy, in such a way that the center of each strip lies

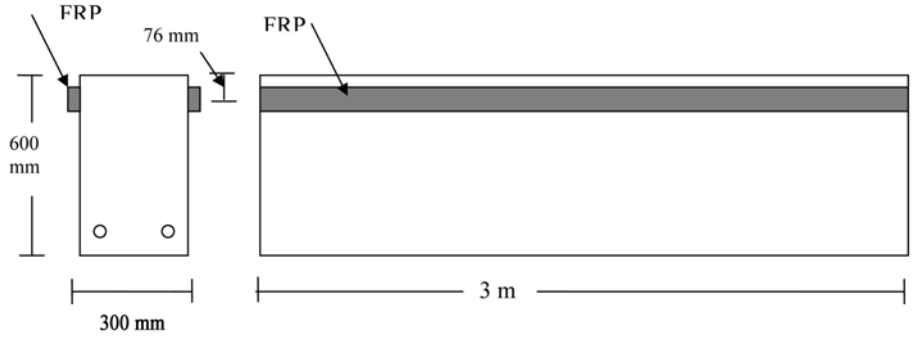

Fig. 4 Layout of FRP fabrics

at 76 mm, concrete cover, from the outer tensile concrete surface as shown in Fig. 4.

Initially, a transverse load of 86.74 kN has been placed at the end of the cantilever to create an ultimate moment at the fixed end. A comparison of the displacements and curvatures along the length of the cantilever for the section reinforced with steel and with FRP systems is presented in Fig. 5. The section is assumed to be uncracked and therefore, concrete contributes in resisting tension. The displacement and curvature behavior of the nonlinear fibers are very close whereas those of the linear fibers are almost identical. The higher values of displacement for the section reinforced with FRP systems is expected since their moduli of elasticity are much lower than that of reinforcing steel. The moduli of elasticity of the FRP systems ranges from 11.7 to 48.3 GPa whereas that of reinforcing steel is 200 GPa. Therefore, beams reinforced with FRP, in general, of reinforcing steel. The moduli of elasticity of the FRP systems ranges from 11.7 to 48.3 GPa whereas that of reinforcing steel is 200 GPa. Therefore, beams reinforced with FRP, in general, offer a much higher deflection than those reinforced with steel. This is also observed with the gradual drop in the curvature in FRP systems compared to the sharp change within the first element

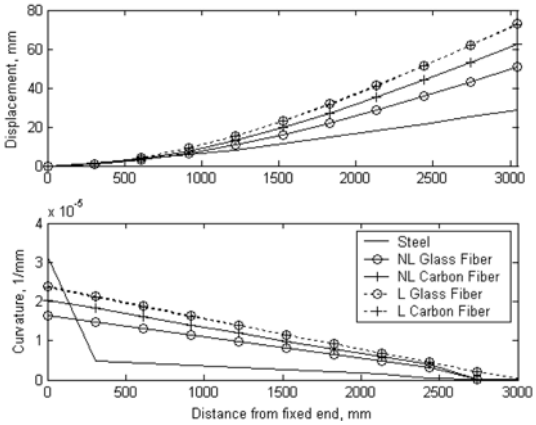

Fig. 5 Displacement and curvature along the length of the cantilever for the steel and FRP systems. Transverse load = 86.740 kN

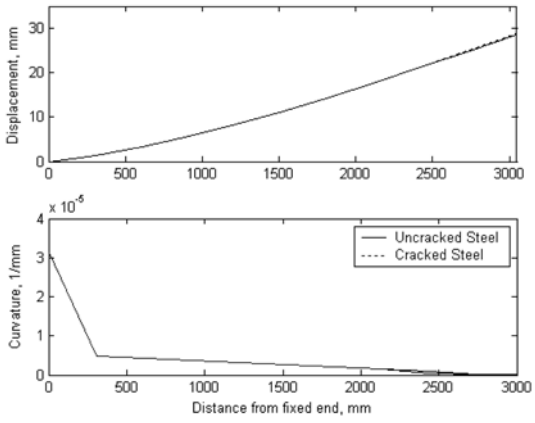

Fig. 6 Displacement and curvature along the length of the cantilever for the steel with alternated cracks and uncracked sections. Transverse load = 86.740 kN

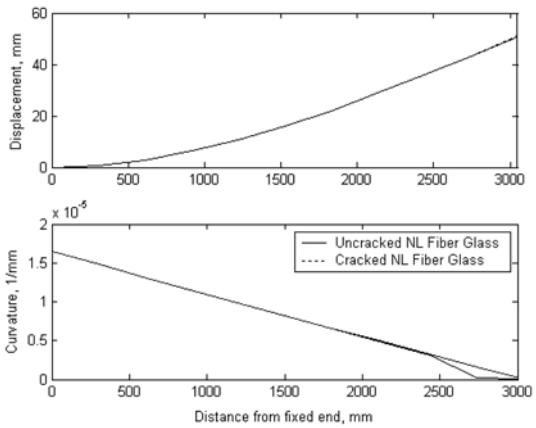

Fig. 7 Displacement and curvature along the cantilever for the nonlinear glass fiber, uncracked and totally cracked. Transverse load = 86.740 kN

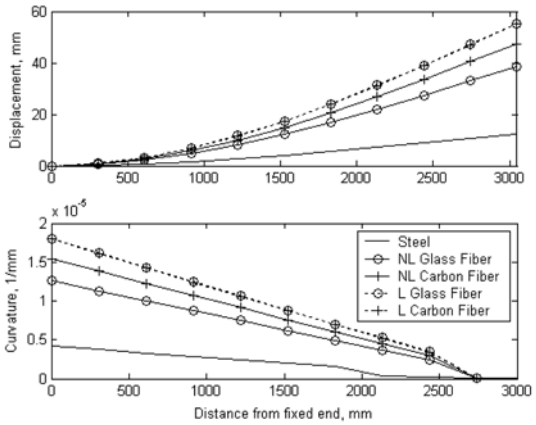

Fig. 8 Displacement and curvature along the length of the cantilever for the steel and FRP systems. Transverse load = 66.723 kN

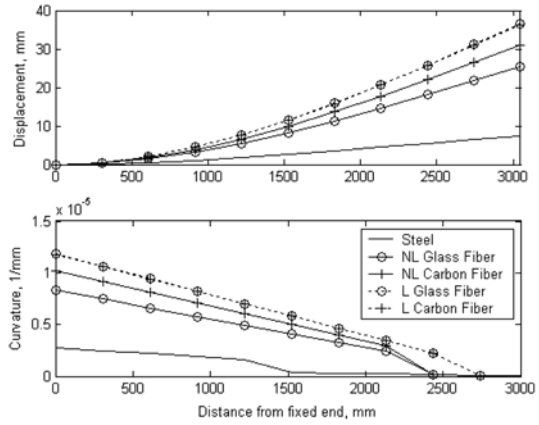

Fig. 9 Displacement and curvature along the length of the cantilever for the steel and FRP systems. Transverse load = 44.482 kN

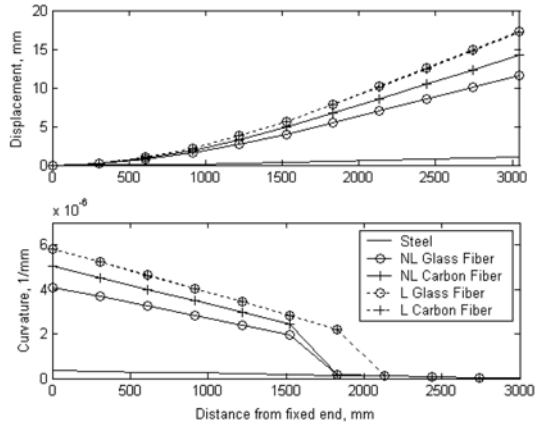

Fig. 10 Displacement and curvature along the length of the cantilever for the steel and FRP systems. Transverse load = 22.241 kN

of the beam. This latter change can be further smoothened, in general, if the finite difference mesh is refined by increasing the number of element. However, it was observed that little difference has taken place by refining the mesh. The mesh utilized in this work consisted of ten elements and eleven nodes.

With the maximum transverse load maintained at 86.74 kN, an analysis has been performed on the effect of patterns of cracking on the displacement and curvature of the beam. Fig. 6 shows a comparison between the behavior of the beam with steel reinforcement and with uncracked and cracked sections at alternated nodes. Fig. 7 presents a comparison between the displacement and curvature behavior of the section, uncracked and totally cracked, reinforced with nonlinear fiber glass. Both figures indicate that cracking slightly increases displacement and curvature. This slight increase is more noticed in sections reinforced with tension steel than in those reinforced with FRP systems.

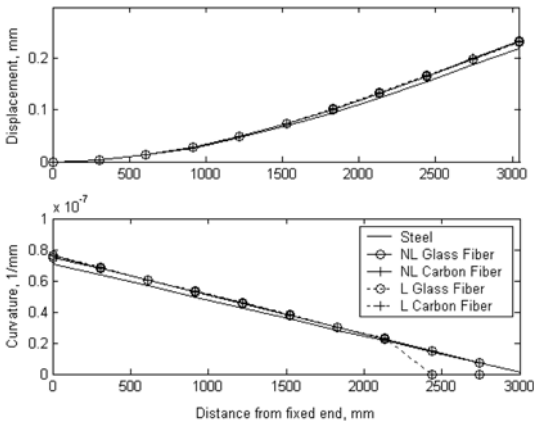

Fig. 11 Displacement and curvature along the length of the cantilever for the steel and FRP systems. Transverse load = 4.448 kN

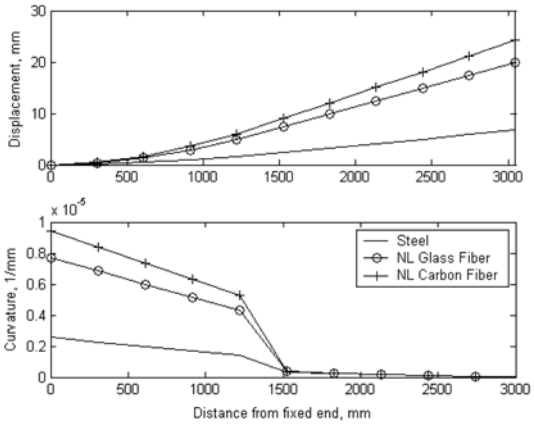

Fig. 12 Displacement and curvature along the length of the cantilever for the steel and FRP systems. Transverse load = 44.282 kN & axial load = -22.241 kN

Figs. 8 to 11 illustrate the displacement and curvature behavior of the cantilever reinforced with steel and FRP systems loaded at the free end with 66.723, 44.482, 22.241 and 4.448 kN respectively. The same difference, as in the ultimate case, between the behavior of the sections reinforced with steel and those with FRP systems with the latter being considerably more ductile. However, the sharp drop in the curvature of sections reinforced with tensile steel observed at the ultimate load case disappears in all other load cases. Also, at 4.448 kN, in Fig. 11, this difference is significantly reduced and the section reinforced with steel approaches those reinforced with FRP systems. Whereas the displacement and curvature of the sections reinforced with FRP systems coincide. This behavior is hardly surprising since at very low loads the curvature at the nodes close to the fixed end are small anyway for all reinforcement types and therefore will not cause large difference in the displacement at the free end. Whereas, at higher loads, the difference in the curvature is very large between steel and FRP reinforcement which will eventually add up to cause a high difference in the displacement at the free end.

A transverse load of 44.482 kN was coupled with an axial compression of 22.241 kN at the free and, the results are shown in Fig. 12 for sections reinforced with steel and nonlinear FRP systems. Comparing the results to those in Fig. 9 where only a transverse load of 44.482 kN was applied, a slight decrease in the displacement and curvature are observed.

6. Conclusions

The following conclusions and recommendations are extracted from the study presented above:

1. The developed technique is based on establishing a load-deflection relationship for sections subjected to combined axial force and bending moment. Material and geometric non-linearities are considered in the method. Elastic-plastic constitutive relations are adopted for material non-linearities. The geometric nonlinearly is solved using a finite difference approach to predict the updated deflected shape of the beam in a step-by-step iteration procedure.

2. The numerical method described in this research has been developed using a PC version of MATLAB. The developed code is accurate, fast and user-friendly. Also, it is easily expandable to include advanced material properties. This latter feature is important when compared to other FEM methods where the researcher is usually restrained by modules and constitutive relations provided by the software house thus hindering further development.

3. FRP fabrics may be utilized as external reinforcement for concrete beams. The FRP reinforced beams were found to possess more ductility than steel reinforced ones.

4. The type and orientation of FRP fabrics greatly affect the behavior and the load carrying capacities of members as they affect the material nonlinearities and hence the constitutive relations parameters.

5. The authors are investigating the properties of additional types of FRP systems as a replacement of tensile steel reinforcement or for use in the repair of structures. Those new types of FRP are usually obtained by either using new materials altogether or by varying the layout and orientation of the fibers in the mesh of the FRP.

6. The developed modules can incorporate a combination of different FRP layers to accommodate specified strength and/or ductility conditions and may also allow for non-uniform sections and different support conditions.

7. The use of FRP systems as a replacement to reinforcing steel is still relatively recent and the model presented in this research study is a modest attempt to advance the understanding of the flexural behavior of such members.

References

ACI committee 440 (1996), "state of the art report on FRP for concrete structures", ACI440R-96, *Manual of Concrete Practice, American Concrete Institute,* MI.

Ahmad, S. H. and Shah, S. P. (1979), "Complete stress- strain curve of concrete and nonlinear design", *CSCE-ASCE-ACI-CEB International Symposium*, University of Waterloo, Ontario, Canada, Aug.

Auciello, N. M. and Ercolano, A. (1992), "Nonlinear analysis of beam subjected to axial and transverse loads", *Comput. Struct.* **44**(4), 863-868.

Bencardino, F., Spadea, G. and Swamy, R. N. (2002), "Strength and ductility of reinforced concrete beams externally reinforced with carbon fiber fabric", *ACI Struct. J.*, **99**(2).

Brena, S. and Macri, B. (2004) "Effect of carbon-fiber reinforced polymer laminate configuration on the behavior of strengthened reinforced concrete beams", *Composites for Construction*, **8**(3).

Desayi, P. and Krishnan, S. (1964), "Equation for the stress-strain curve of concrete", *ACI J. Struct. Eng., Proc.* **61**, 345-350.

Duthinh, D. and Starnes, M. (2004), "Strength and ductility of concrete beams reinforced with carbon fiber-reinforced polymer plates and steel", *Composites for Construction,* **8**(1).

El-Hawary, M. M., Fereig, S., Al-Duaij, J. and Al-Khaiat, H. (2003), "On the retrofitting of RC beams using FRP fabrics", *First International Conference of the ACI Kuwait Chapter, Kuwait*, September.

Fertis, D. G. and Keene, Michael E. (1990), "Elastic and inelastic analysis of nonprismatic members", *J. Struct. Eng.* ASCE, **116**(2), Feb.

Fertis, D. G. and Tanej Rajesh (1991), "Equivalent systems for inelastic analysis of prismatic and nonprismatic members", *J. Struct. Eng.* ASCE, **117**(2), Feb.

Fertis, D. G. and Zobel, E. (1958), "Equivalent system for the deflection of variable stiffness members", *J. Struct. Div.*

Fertis, D. G. and Zobel, E. (1961), *Transverse vibration theory, application of equivalent systems,* Roland Press Co., Inc. New York, N. Y.

Fujikake, K., Mindess, S. and Xu, H. (2004), "Analytical model for concrete confined with fiber reinforced polymer composite", *Composites for Construction,*, **8**(4).
Hamid, A. Issa, M., Sabouni, A. R. and Mukhtar, A. (1995), "Use of fiber reinforced plastics in reinforced concrete slabs", *Proceedings of the Sixth Arab Structural Engineering Conference,* Damascus University, Damascus, Syria.
Hamoush, S. (2001), "Upgrading of non-ductile reinforced concrete frame connections with FRP overlay systems" *Final Report, Army Corps of Engineers* (CREL), May.
Hamoush, S. A. and Terro, M. J. (1993), "Inelastic analysis of sections subjected to axial force and bending moment", *Comput. Struct*.
Javier Malvar, L., Morrill, K. and Crawford, J. (2004), "Numerical modeling of concrete confined by fiber-reinforced composites", *Composites for Construction,* **8**(4).
MATLAB 6.5, Release 13, The Mathworks, Inc., Natick, Massachusetts, USA, 2002.
Ngo, D. and Scordelis, A. C. (1967), Finite element analysis of reinforced concrete beams", *ACI J.,* **64**(3), 152-163.
Pagnoni, T. and Slater, J. (1992), "A nonlinear three dimensional analysis of reinforced concrete based on a bounding surface model", *Comput. Struct.*, **43**(1), 1-12.
Rasheed, H. A. S. and Dinno, K. S. (1994), "An efficient nonlinar analysis of RC sections", *Comput. Struct.* **53**(3), 613-623.
Spadea, G., Bencardino, F. and Swamy, R. N. (2000), "Optimizing the performance characteristics of beams strengthened with bonded CFRP laminates", *Mater. and Struct.*, **33**.
Swamy, R. N. and Mukhopadhyaya, P. (1999), "Debonding of carbon-fiber-reinforced polymer plate from concrete beams", *Struct. Bldg.*, **134**.
Tsai, Wan T. (1987), "Uniaxial stress-strain relation of concrete", *J. Struct. Eng.* ASCE, **114**(9).
Vecchio, Frank J. (1989), "Nonlinear finite element analysis of reinforced membranes". *ACI Struct. J.*, Jan- Feb.
Wang, P. T., Shah, S. P. Naaman, A. E. (1978), "Stress-strain curves of normal and lightweight concrete in compression", *ACI Struct. J.*, Nov.

CC